Molecular Mechanics Study of the Ruffling of Metalloporphyrins

Orde Q. Munro, Julia C. Bradley, Robert D. Hancock,* Helder M. Marques,* Fabrizio Marsicano, and Peter W. Wade

Contribution from the Centre for Molecular Design, Department of Chemistry, University of the Witwatersrand, Wits 2050, Johannesburg, South Africa. *Received November 8, 1991*

Abstract: Molecular mechanics techniques using a modified version of the program MM2(87) were used to analyze the ruffling of metalloporphyrins as a function of metal ion size, orientation of axial ligands, and orientation of substituents on the porphyrin periphery. The structures chosen for the parametrization, $[P(TPP)(OH)_2]^+$, the planar and ruffled forms of low-spin (S = 0) [Ni(OEP)], (S = 1) [Fe(TPP)], [Zn(TPP)], and [Pb(TPrP)], contain metal ions of very different sizes and hence extents of porphyrin core ruffling. The planar and moderately ruffled structures could be satisfactorily reproduced by developing new parameters involving the metal ion and using the parameters built into the program for the porphyrin core. The total strain energy in a planar metalloporphyrin was investigated as a function of metal ion size. The principal components which contribute to the total strain energy are nonbonded van der Waals repulsion, bond angle deformation, and bond length deformation. A minimum in the strain energy curve occurs at 2.035 Å which is the best-fit metal ion size in the planar macrocycle cavity. In the case of the very small ion, P(V), only a ruffled conformer is possible, but for intermediate size metal ions (Ni(II) and Fe(II)) both planar and ruffled forms of the metalloporphyrins were found (in accord with the experimental observation of the two forms of [Ni(OEP)] in solution and in the solid state). As ruffling increases, there is a balance between a decrease in bond length deformation and angle bending strain, and an increase in torsional strain, such that the energy difference between the two forms is small with the planar structure 1-1.5 kcal·mol^{-1} more stable. For the larger ion, Zn(II), only the planar form was found, and for the very large ion, Pb(II), a domed structure results in which the coordination geometry is best described as square pyramidal. The flexibility of the porphyrin core was further demonstrated by showing that at the expense of a modest 1.3 kcal·mol^{-1} (arising principally from an increase in angle bending strain) the porphyrin ring can undergo a cavity expansion of 0.15 Å and accommodate a change in the spin state of Fe(II) from low spin to high spin without requiring the metal ion to be extruded out of the mean plane. The ruffling of a metalloporphyrin is normally either of the *sad* or *ruf* variety, and the sense and extent of the ruffling is demonstrated to be controlled by the specific orientations of phenyl groups in TPP complexes and by the orientation of ligands such as 2-methylimidazole coordinated to the axial sites of the metal ion. Some examples of the ruffling of porphyrins in hemoproteins in response to their environment are considered.

There is considerable evidence to indicate that the conformations of metalloporphyrin and free-base tetrapyrrole prosthetic groups may have a profound influence on the physical and chemical properties of the macrocycle and therefore its reactivity in a protein. For example, the reactions catalyzed by vitamin B_{12} are thought to be influenced by the conformation of the cobalt corrinoid;[1] the extent of macrocycle ruffling of the nickel-containing cofactor F_{430} from methyl reductase determines the affinity of the metal ion for added ligands and therefore aspects of its reactivity;[2-7] ruffled conformations of (bacterio)chlorophylls and chlorins, observed crystallographically for both the free and bound cofactors,[8-17] may control the electronic and redox properties of these prosthetic groups through modulation of the relative energies of the frontier molecular orbitals of the chromophore.[18-20] Domed and ruffled heme group conformations have been observed in the crystal structures of many hemoproteins,[21-30] and there has been considerable interest in the functional significance of such prosthetic group conformations, particularly in relation to the mechanism of hemoglobin cooperativity.[31-35] It is generally difficult to delineate clearly the factors responsible for heme group conformations because of the multitude of interactions with amino acid residues within the heme-binding pocket(s) of the protein.[21-31]

A wealth of structural information[36,37] relating to the stereo-

(1) Geno, M. K.; Halpern, J. *J. Am. Chem. Soc.* **1987**, *109*, 1238.
(2) Eschenmoser, A. *Ann. N.Y. Acad. Sci.* **1986**, *471*, 108.
(3) Shellnut, J. A. *J. Am. Chem. Soc.* **1987**, *109*, 4169.
(4) Shellnut, J. A. *J. Phys. Chem.* **1989**, *93*, 6283.
(5) Crawford, B. A.; Findsen, E. W.; Ondrias, M. R. *Inorg. Chem.* **1988**, *27*, 1842.
(6) Shiemke, A. K.; Scott, R. A.; Shellnut, J. A. *J. Am. Chem. Soc.* **1988**, *110*, 1645.
(7) Shiemke, A. K.; Kaplan, W. A.; Hamilton, C. L.; Shellnut, J. A.; Scott, R. A. *J. Biol. Chem.* **1989**, *264*, 7276.
(8) Barkigia, K. M.; Fajer, J.; Smith, K. M.; Williams, G. J. B. *J. Am. Chem. Soc.* **1981**, *103*, 5890.
(9) Strouse, C. E. *Proc. Natl. Acad. Sci. U.S.A.* **1974**, *71*, 325.
(10) Kratky, C.; Dunitz, J. D. *Acta Crystallogr., Sect. B* **1975**, *B32*, 1586; **1977**, *B33*, 545.
(11) Barkigia, K. M.; Fajer, J.; Chang, C. K.; Young, R. *J. Am. Chem. Soc.* **1984**, *106*, 6457.
(12) Chow, H. C.; Serlin, R.; Strouse, C. E. *J. Am. Chem. Soc.* **1975**, *97*, 7230.
(13) Serlin, R.; Chow, H. C.; Strouse, C. E. *J. Am. Chem. Soc.* **1975**, *97*, 7237.
(14) Kratky, C.; Dunitz, J. D. *J. Mol. Biol.* **1977**, *113*, 431.
(15) Kratky, C.; Isenring, H. P.; Dunitz, J. D. *Acta Crystallogr., Sect. B* **1977**, *B33*, 547.
(16) Tronrud, D. E.; Schmid, M. F.; Mathews, B. W. *J. Mol. Biol.* **1986**, *188*, 443.
(17) Michel, H.; Epp, O.; Deisenhofer, J. *EMBO J.* **1986**, *5*, 2445.
(18) Nakasuji, K.; Yamaguchi, M.; Murata, I. *J. Am. Chem. Soc.* **1986**, *108*, 323.
(19) Barkigia, K. M.; Chantranupong, L.; Smith, K. M.; Fajer, J. *J. Am. Chem. Soc.* **1988**, *110*, 7566.
(20) Alden, R. G.; Crawford, B. A.; Doolen, R.; Ondrias, M. R.; Shelnutt, J. A. *J. Am. Chem. Soc.* **1989**, *111*, 2070.
(21) Takano, T. *J. Mol. Biol.* **1977**, *110*, 537.
(22) Deatherage, J. F.; Loe, R. S.; Anderson, C. M.; Moffat, K. *J. Mol. Biol.* **1976**, *104*, 687.
(23) Ladner, R. C.; Heidner, E. J.; Perutz, M. F. *J. Mol. Biol.* **1977**, *114*, 385.
(24) Takano, T.; Dickerson, R. E. *J. Mol. Biol.* **1981**, *153*, 95.
(25) Takano, T.; Dickerson, R. E. *J. Mol. Biol.* **1981**, *153*, 79.
(26) Louie, G. V.; Brayer, G. D. *J. Mol. Biol.* **1990**, *214*, 527.
(27) Bushnell, G. W.; Louie, G. V.; Brayer, G. D. *J. Mol. Biol.* **1990**, *214*, 585.
(28) Ochi, H.; Hata, Y.; Tanaka, N.; Kakudo, M.; Sakurai, T.; Aihara, S.; Morita, Y. *J. Mol. Biol.* **1983**, *166*, 407.
(29) Wang, J.; Mauro, J. M.; Edwards, S. L.; Oatley, S. J.; Fishel, L. A.; Ashford, V. A.; Xuong, N.; Kraut, J. *Biochemistry* **1990**, *29*, 7160.
(30) Edwards, S. L.; Poulos, T. L. *J. Biol. Chem.* **1990**, *265*, 2588.
(31) Antonini, E.; Brunori, M. In *Hemoglobin and Myoglobin in their Reactions with Ligands*; Neuberger, A., Tatum, E. L., Eds.; North-Holland Publishing Company: Amsterdam, 1971; pp 73-89.
(32) Hoard, J. L.; Scheidt, W. R. *Proc. Natl. Acad. Sci. U.S.A.* **1973**, *70*, 3919.
(33) Hoard, J. L.; Scheidt, W. R. *Proc. Natl. Acad. Sci. U.S.A.* **1974**, *71*, 1578.
(34) Perutz, M. F. *Proc. R. Soc. London, Ser. B* **1980**, *208*, 135.
(35) Scheidt, W. R.; Reed, C. A. *Chem. Rev.* **1981**, *81*, 543.
(36) Hoard, J. L. In *Porphyrins and Metalloporphyrins*; Smith, K. M., Ed.; Elsevier Scientific Publishing Company: Amsterdam, 1975; Chapter 8.
(37) Scheidt, W. R.; Lee, Y. J. *Struct. Bonding* **1987**, *64*, 1.

0002-7863/92/1514-7218$03.00/0

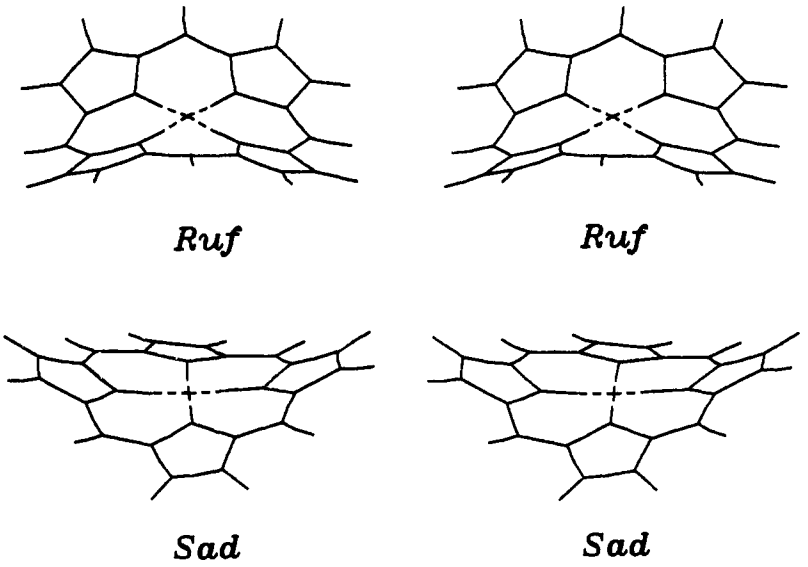

Figure 1. Stereoview of MM2-generated *sad* and *ruf* forms of ruffled metalloporphyrins. For clarity, peripheral substituents have been replaced with hydrogen atoms and axial ligands removed.

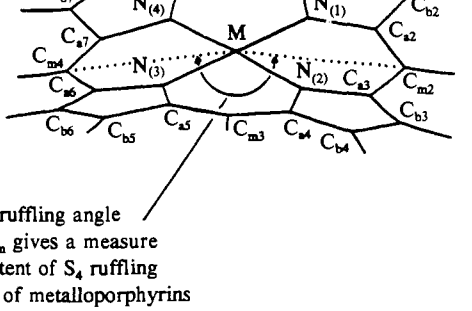

Figure 2. The atom-labeling scheme for the metalloporphyrins used in this work. The extent of S_4 ruffling of the *ruf* form of a metalloporphyrin may be characterized either by the ruffling angle (C_m–M–C_m) or by the average absolute displacement of the four *meso* carbon atoms (C_m) from the mean plane of the 25-atom metalloporphyrin core.

chemistry of both synthetic and naturally occurring simple metalloporphyrin complexes indicates that ruffled conformations are not unique to hemoproteins. This suggests that the observed conformation of a metalloporphyrin prosthetic group is not exclusively dependent on the constraints imposed by the binding site of the protein.

The D_{2d} ruffling of a porphyrin leads to one of two core conformations termed *ruf* and *sad* (Figure 1).[37] In the *ruf* form, opposite pyrrole rings are counterrotated so that the *meso* (C_m) carbon atoms of each pyrrole ring are alternately displaced above and below the mean porphyrin plane. In the *sad* form, each of the pairs of C_b carbon atoms forming the outer edge of each pyrrole ring are alternately displaced above and below the mean porphyrin plane, while the C_m carbon atoms are approximately in the mean porphyrin plane (see Figure 2 for nomenclature). Both planar and S_4-ruffled conformations of [Ni(OEP)][38] have been observed in the crystalline solid state[39,40] and in solution,[20] while many other square-planar metalloporphyrins crystallize with S_4-ruffled core conformations. These include (S = 1) [Fe(TPP)],[41] [Co(TPP)],[42] [Cu(TPP)],[43] [Pd(TPP)],[43] and [Pt(TPP)].[44] In addition, a range of 6-coordinate S_4-ruffled species are known, such as $[P(TPP)(OH)_2]OH$,[45] $[Fe(TPP)(2\text{-MeIm})_2]ClO_4$,[46] and $[Fe(TPP)(Im)_2]Cl$.[47] For larger square-planar metal ions, planar conformations exhibiting C_i symmetry are common, for example [Zn(TPP)][48] and [Ag(TPP)].[49] Very large metal ions tend toward a square-pyramidal coordination geometry, as in [Pb(TPrP)][50] and 5-coordinate high-spin ferrous and ferric porphyrins.[35] On the basis of X-ray structural data, it has been suggested[36,37] that the metalloporphyrin core conformation responds to the dictates of the specific metal–nitrogen (M–N) bonding requirements in the macrocycle.

The *sad* core conformation is unique to $[M(TPP)]^{n+}$ complexes[37] and may be associated with the effects of crystal lattice forces on the orientations of the peripheral phenyl substituents. The conformation, however, is not confined to the solid state, since [M(TPP)] complexes with sterically crowded peripheral alkyl substituents are locked into this core geometry even in solution.[19,51,52]

Molecular mechanics (MM) techniques have been used to investigate structural features of metalloporphyrins. We have communicated a preliminary report;[53] Kollman et al.[54] have re-

(38) Abbreviations: HS, high-spin; Im, imidazole; L, a ligand donor atom; LFSE, ligand field stabilization energy; LS, low-spin; M, a metal ion; 1-MeIm, 1-methylimidazole; 2-MeIm, 2-methylimidazole; 4-MeIm$^-$, 4-methylimidazolate; 4-MePip, 4-methylpiperidine; MM, molecular mechanics; OEP, 2,3,7,8,12,13,17,18-octaethylporphyrin; P, porphine; Ph, phenyl; PMS, pentamethylene sulfide; porph, a porphyrin; PPIX, protoporphyrin-IX; SC_6HF_4, 2,3,5,6-tetrafluorobenzene thiolate; TAP, 5,10,15,20-tetrakis(*p*-methoxyphenyl)porphyrin; TPP, 5,10,15,20-tetraphenylporphyrin; TPP-C_3Im, 5-mono[2-(5-(*N*-imidazolyl)valeramido)-1-phenyl]-10,15,20-triphenylporphyrin; TPrP, 5,10,15,20-tetra-*n*-propylporphyrin; TPyP, 5,10,15,20-tetra(4-pyridyl)porphyrin.

(39) Meyer, E. F. *Acta Crystallogr., Sect. B* **1972**, *28*, 2162.
(40) Cullen, D. L.; Meyer, E. F. *J. Am. Chem. Soc.* **1974**, *96*, 2095.
(41) Collman, J. P.; Hoard, J. L.; Kim, N.; Lang, G.; Reed, C. A. *J. Am. Chem. Soc.* **1975**, *97*, 2676.
(42) Madura, P.; Scheidt, W. R. *Inorg. Chem.* **1976**, *15*, 3182.
(43) Fleischer, E. B.; Miller, C. K.; Webb, L. E. *J. Am. Chem. Soc.* **1964**, *86*, 2342.
(44) Hazell, A. *Acta Crystallogr., Sect. C* **1984**, *C40*, 751.
(45) Mangani, S.; Meyer, E. F.; Cullen, D. L.; Tsutsui, M.; Carrano, C. J. *Inorg. Chem.* **1984**, *22*, 400.
(46) Scheidt, W. R.; Kirner, J. F.; Hoard, J. L.; Reed, C. A. *J. Am. Chem. Soc.* **1987**, *109*, 1963.
(47) Collins, D. M.; Countryman, R.; Hoard, J. L. *J. Am. Chem. Soc.* **1972**, *94*, 2066.
(48) Scheidt, W. R.; Kastner, M. E.; Hatano, K. *Inorg. Chem.* **1978**, *17*, 706.
(49) Scheidt, W. R.; Mondal, J. U.; Eigenbrot, C. W.; Adler, A.; Radonovich, J. L.; Hoard, J. L. *Inorg. Chem.* **1986**, *25*, 795.
(50) Barkigia, K. M.; Fajer, J.; Adler, A. D.; Williams, G. J. B. *Inorg. Chem.* **1980**, *19*, 2057.
(51) Medforth, C. J.; Berber, M. D.; Smith, K. M.; Shelnutt, J. A. *Tetrahedron Lett.* **1990**, *31*, 3719.
(52) Shelnutt, J. A.; Medforth, C. J.; Berber, M. D.; Barkigia, K. M.; Smith, K. M. *J. Am. Chem. Soc.* **1991**, *113*, 4077.
(53) Hancock, R. D.; Weaving, J. S.; Marques, H. M. *J. Chem. Soc., Chem. Commun.* **1989**, 1176.
(54) (a) Lopez, M. A.; Kollman, P. A. *J. Am. Chem. Soc.* **1989**, *111*, 6212. (b) Kollman, P. A.; Grootenhuis, P. D. J.; Lopez, M. A. *Pure Appl. Chem.* **1989**, *61*, 593.

ported models aimed at establishing the interaction of carbon monoxide and dioxygen with ferrous porphyrins; and Shelnutt et al.[52] have correlated the core sizes of ruffled synthetic nickel porphyrins with the positions of structure-sensitive Raman lines using X-ray crystallographic and MM structural data. We report here on the development of a force field for a modified version of the program MM2(87)[55] for analyzing factors affecting metalloporphyrin conformations: (i) the effect of the size of the metal ion coordinated by the porphinato ligand; (ii) the effect of axial ligation by planar ligands such as imidazoles; (iii) the effect of phenyl group orientation in $[M(TPP)]^{n+}$ complexes; and (iv) the flexibility of the porphyrin macrocycle.

We chose MM2 for our calculations as the program has already been used in calculations on transition-metal complexes of macrocycles[56-59] and chelates[60] and on lanthanide coordination complexes.[61] Furthermore, it has been designed to model conjugated heterocyclic π-systems, an important consideration when modeling tetrapyrrole macrocycles.

There are currently two approaches used to represent metal–ligand (M–L) bonds in MM calculations.[62,63] In the "bonded" approach the M–L bond is treated as a covalent bond and is defined by ideal bond lengths and angles, with appropriate force constants. In the "nonbonded" approach the M–L bond is treated using electrostatic and van der Waals forces. The choice of model depends on the nature of the problem to be investigated, with each approach having distinct advantages in different situations.

In the "nonbonded" MM approach to M–L bonds the number and identity of the coordinated ligands can vary during structural refinement so that, for example, a 4-coordinate metal ion may become 5-coordinate,[62] therefore allowing *dynamic* simulation of substrate binding; the coordination geometry is determined largely by the nature and steric requirements of the ligands interacting with the metal ion, and the inherently flexible inner coordination sphere permits configurational rearrangements.[62] This is not an essential requirement for simulating complexes of well-defined symmetry where only small or moderate distortions in coordination geometry are required, and which have usually been modeled within the framework of the "bonded" formalism.[56-58,64-68]

One of the problems that arises with the "nonbonded" approach is the derivation of electrostatic parameters for the ligands and for the M–L bonds. In particular, poor transferability of force field parameters between models[69,70] results from uncertainty in the choice of dielectric constant[71-73] and in the estimation of charge partitioning[74,75] between atom pairs in the ligands and the M–L bonds.[62,76] Although a variety of computational methods have been used to determine charge partitioning between bonded atoms in principally organic moieties,[69,70,77-80] there seem to be no well-established methods for determining transition-metal M–L dipoles. Force field parametrizations for alkali metal cations have prompted theoretical strategies to overcome problems involving the polarization effects of the cation, such as inclusion of bond[81,82] polarizabilities in the empirical energy function, but an extension to transition-metal cations has not yet been attempted. Several approximations for complexes of transition-metal ions, predominantly in "bonded" MM models that include electron distribution effects, are accordingly found; these range from setting the M–L dipoles to zero and excluding charges to arbitrary choices of parameters.[52,56-59,61,64-68,86] Electrostatic parameters for metal–ligand interactions will obviously be more critical in the "nonbonded" approach,[62] and a recent strategy, in which dynamic adjustment of charge distribution in the M–L bonds during conformational optimization is effected, has improved the reliability of calculations for metal ions in proteins.[62] However, it is interesting to note that in several instances there are only minor differences in the results, arising from small variations in, or the neglect of, electrostatic parameters.[87-89]

Most currently used force fields, including MM2[54] and AMBER,[90] contain potential functions which take into account electron distribution phenomena, in addition to treating bond lengths and angles by standard quadratic or related potential functions. The use of electrostatic (or dipole) parameters is therefore optional with these force fields. Older force fields that have been used to model complexes of transition-metal ions, and which do not feature electrostatic potentials (e.g., MOLBLD[91]), may be considered as strictly "bonded" MM approaches. The following advantages are offered by the covalent approach to M–L bonding: (i) the effects of charge partitioning in the M–L bonds can be attenuated or ignored since this contribution to the observed M–L bond in the real molecule is nonspecifically accounted for by the parametrized quadratic or cubic bond compression function in the force field;[92] (ii) in tetraaza macrocycles l_o for HS and LS

(55) (a) Allinger, N. L. *J. Am Chem. Soc.* **1977**, *99*, 8127. (b) Allinger, N. L.; Yuh, Y. MM2(87). Distributed to academic users by QCPE, under special agreement with Molecular Design Ltd., San Leandro, CA.
(56) Drew, M. G. B.; Yates, P. C. *J. Chem. Soc., Dalton Trans.* **1987**, 2563.
(57) Schwarz, C. L.; Endicott, J. F. *Inorg. Chem.* **1989**, *28*, 4011.
(58) Endicott, J. F.; Kumar, K.; Schwarz, C. L.; Perkovic, M. W.; Lin, W.-K. *J. Am. Chem. Soc.* **1989**, *111*, 7411.
(59) Adam, K. R.; Antolovich, M.; Brigden, L. G.; Lindoy, L. F. *J. Am. Chem. Soc.* **1991**, *113*, 3346.
(60) Yoshikawa, Y. *J. Comput. Chem.* **1990**, *11*, 326.
(61) Ferguson, D. M.; Raber, D. J. *J. Comput. Chem.* **1990**, *11*, 1061.
(62) Vedani, A.; Huhta, D. W. *J. Am. Chem. Soc.* **1990**, *112*, 4795.
(63) Sabolović, J.; Raos, N. *Polyhedron* **1990**, *9*, 2419.
(64) Brubaker, G. R.; Johnson, D. W. *Coord. Chem. Rev.* **1984**, *53*, 1 and references therein.
(65) Hambley, T. W.; Hawkins, C. J.; Palmer, J. A.; Snow, M. R. *Aust. J. Chem.* **1981**, *34*, 2525.
(66) Hambley, T. W. *J. Chem. Soc., Dalton Trans.* **1986**, 565.
(67) McDougall, G. J.; Hancock, R. D.; Boeyens, J. C. A. *J. Chem. Soc., Dalton Trans.* **1978**, 1438.
(68) Thöm, V. J.; Fox, C. C.; Boeyens, J. C. A.; Hancock, R. D. *J. Am. Chem. Soc.* **1984**, *106*, 5947.
(69) Price, S. L.; Faerman, C. H.; Murray, C. W. *J. Comput. Chem.* **1991**, *12*, 1187.
(70) Bruning, H.; Feil, D. *J. Comput. Chem.* **1991**, *12*, 1.
(71) Adams, M. D.; Wade, P. W.; Hancock, R. D. *Talanta* **1990**, *37*, 875.
(72) Bovill, M. S.; Chadwick, D. J.; Sutherland, I. O. *J. Chem. Soc., Perkin Trans.* **1980**, *2*, 1529.
(73) Vedani, A.; Dobler, M.; Dunitz, J. D. *J. Comput. Chem.* **1986**, *7*, 701.
(74) Wipff, G.; Weiner, P.; Kollman, P. *J. Am. Chem. Soc.* **1982**, *104*, 3249.
(75) Kollman, P.; Wipff, G.; Singh, U. C. *J. Am. Chem. Soc.* **1985**, *107*, 2212.
(76) Vedani, A.; Huhta, D.; Jacober, S. P. *J. Am. Chem. Soc.* **1989**, *111*, 4075.
(77) Bartolotti, L. J.; Pederson, L. G.; Charifson, P. S. *J. Comput. Chem.* **1991**, *12*, 1125.
(78) Mullay, J. *J. Comput. Chem.* **1991**, *12*, 369.
(79) Ferenczy, G. G. *J. Comput. Chem.* **1991**, *12*, 913.
(80) Cieplak, P.; Kollman, P. *J. Comput. Chem.* **1991**, *12*, 1232.
(81) Ortega-Blake, I.; Lēs, A.; Rybak, S. *J. Theor. Biol.* **1983**, *104*, 571.
(82) Clementi, E.; Kistenmacher, H.; Kolos, W.; Romano, S. *Theor. Chim. Acta* **1980**, *55*, 257.
(83) Åqvist, J.; Warshel, A. *Biochemistry* **1989**, *28*, 4680.
(84) Lybrand, T. P.; Kollman, P. A. *J. Chem. Phys.* **1985**, *83*, 2923.
(85) Sussman, F.; Weinstein, H. *Proc. Natl. Acad. Sci. U.S.A.* **1989**, *86*, 7880.
(86) Hambley, T. W. *Inorg. Chem.* **1991**, *30*, 937.
(87) Damu, K. V.; Hancock, R. D.; Wade, P. W.; Boeyens, J. C. A.; Billing, D. G.; Dobson, S. M. *J. Chem. Soc., Dalton Trans.* **1991**, 293.
(88) Ragazzi, M.; Ferro, D. R.; Provasoli, A. *J. Comput. Chem.* **1986**, *7*, 105.
(89) Clark, M.; Cramer, R. D., III; Van Opdenbosch, N. *J. Comput. Chem.* **1989**, *10*, 982.
(90) Weiner, S. J.; Kollman, P. A.; Case, D. A.; Singh, U. C.; Ghio, C.; Alagona, G.; Profeta, S.; Weiner, P. *J. Am. Chem. Soc.* **1984**, *106*, 765.
(91) Boyd, R. H.; Breitling, S. M.; Mansfield, M. *Am. Inst. Chem. Eng. J.* **1973**, *19*, 1016.
(92) M–L strain-free bond lengths and force constants are usually derived to fit structural data obtained by X-ray crystallography. Implicit in these parameters are various contributions (electrostatic forces, anisotropy in electron distribution due to nonequivalent electronegativities and local conformational geometry, σ-bonding effects, and L↔M π-bonding contributions) which lead to the formation of the M–L bond. Useful MM force fields for coordination complexes are therefore possible when these separate effects are accounted for in a nonspecific manner in the potential functions used to simulate the experimentally observed M–L bonds. Similarly, simple analytical functions adequately simulate H-bonding geometries without extensive consideration of charge-transfer or second-order effects (Ferguson, D. M.; Kollman, P. A. *J. Comput. Chem.* **1991**, *12*, 620. Vedani, A.; Dunitz, J. D. *J. Am. Chem. Soc.* **1985**, *107*, 7653).

Ni^{2+} is 2.10 and 1.89 Å, respectively,[68] indicating that specific spin-states of a metal ion in a given oxidation state can be simulated by appropriate selection of strain-free bond lengths (l_o) for the M–L bonds;[93] and (iii) in a similar manner to "nonbonded" formalisms, the covalent model can be extended to complexes where the coordination geometry is determined by the identity and steric requirements of the complexed ligands simply by using 1,3-nonbonded interactions at the metal instead of angle bending parameters for the L–M–L angles.[61]

A significant disadvantage restricting widespread application of the "bonded" model in coordination chemistry is that the number of ligands attached to the metal cannot change during geometry optimization. A *dynamic* simulation of ligand (substrate) binding is therefore beyond the method at present.

To our knowledge, in neither of the two approaches are there reported simulations of *dynamic* changes in the spin-state of a metal ion, which would seemingly require adjustment of the M–L bond compression parameter as well as the intrinsic potential energy (LFSE) of the metal ion. Nonetheless, calculations taking into account changes in LFSE that may arise from configurational reorganization for metal ions in a fixed spin-state have recently been reported.[62]

Despite the use of approximate parameters for metal ions in many MM models, plausible structures, and thermodynamic data, as well as conformational populations correlating with NMR data,[64-68,71] have been reported for various systems, suggesting that electrostatic and nonbonded parameters for the M–L interactions in "bonded" MM approaches are of secondary importance compared to the compression potential for the M–L bonds.

Irrespective of the method used, the predictions made should be in agreement. Recent work on macrocyclic complexes of alkali metal cations and Ni^{2+} has demonstrated that the results obtained with several force field methods are generally in accord on most issues.[59,87]

In this work we have set all dipoles involving the metal ion to zero and treated the metal as an uncharged atom; we have retained the standard MM2 dipole parameters for the porphyrin and axial ligands. The SCF π-MO calculations on all structural subunits having delocalized π-electrons, such as imidazole ligands and the porphyrin macrocycle, were retained. The porphinato ligand provides an essentially invariant set of four coplanar nitrogen donor atoms (N–M–N angles remain fairly close to 90° and 180°, in square-planar and octahedral coordination geometries), which means that the inner coordination sphere of the metal ion is stereochemically less variable than in simple transition-metal complexes, and therefore amenable to treatment in terms of the "bonded" model. The current model is therefore directed at delineation of steric phenomena that may have an effect on the conformation of the porphyrin in metalloporphyrin complexes.

Force field parameters were developed for modeling the bonds and angles involving the metal centers of six porphyrins[39-41,45,48,50] with metal ions of very different sizes, and hence porphyrin cores displaying differing degrees of ruffling. Ten imidazole ferric porphyrin complexes[46,47,94-99] were used for additional parametrization of the force field for LS Fe^{3+}. The structures predicted by MM were in reasonable agreement with the observed crystal structures. Usually MM2(87) appeared to show little tendency to fall into false minima and the same structures could be obtained from different starting trial structures. This was taken as an indication that MM2(87) could be used to analyze the steric factors controlling the ruffling of metalloporphyrins. The work reported here on axial ligation by imidazoles is the result of a preliminary analysis of axial ligand binding to metalloporphyrins, and details will be published elsewhere.

Computational Methods

Programs Used. The MM calculations were carried out using a modified form of the MM2(87) program of Allinger et al.[55] distributed by the Quantum Chemistry Program Exchange (QCPE). (Refer to Appendix for the functions used.) The MM2(87) computer program received from QCPE was the VAX version and consisted of 72 program modules written in FORTRAN. We wrote two subroutines, EXIT and IPACK4, which were missing. All program modules were compiled using an NDP FORTRAN-386 Fortran compiler obtained from MicroWay, Inc. for an IBM-compatible personal computer fitted with an Intel 80386 microprocessor, a 80387 co-processor, and 4Mb RAM. Program modules were linked using the FASTLink linker for the Intel 80386 microprocessor and loaded into extended memory by the 386/DOS-Extender, both obtained from Phar Lap Software, Inc. ALCHEMY II[100] was used to set up molecule data files for MM2 and to plot energy-minimized molecular coordinates obtained from such calculations.

All geometry optimizations were performed with a convergence criterion equivalent to $\Delta E \leq (8 \times 10^{-5})N$ kcal·mol^{-1}, where N is the number of atoms in the molecule and ΔE is the energy difference between successive iterations. No significant structural improvements were obtained with an optimization cut-off of $\Delta E \leq (8 \times 10^{-6})N$ kcal·mol^{-1}.

Modifications to MM2(87). Some program changes of a fairly minor nature were required to program modules DOMGA, DRANG, DOPB1, DOPB2, DOPB3, DIHD, and ROTAT, to avoid memory protection faults arising from arithmetic division by numbers close to, or equal to, zero. One situation that leads to this condition arises when two bonds in a molecular become co-linear, or almost co-linear, as, for example, happens not infrequently in metal–ligand complexes with an octahedral bonding geometry. Other minor changes were required in order to replace some Fortran coding that was not recognized by the compiler used.

In order to carry out the calculations required in this study, and in other studies currently being undertaken in our laboratories involving coordinated metal ions, it was necessary to modify the program to allow it to handle atoms that are more than 4-coordinate. This modification involved increasing the dimensions of a number of variables in common blocks throughout the program and also additional coding to subroutines BONDS, EBEND, KTHETA, THETA, DAVEJR, KBOND, BONDTB, MAIN, and TOTAL. The program currently in use can accommodate up to 8 attachments per atom.

In cases where a metal ion is coordinated to more than one donor atom of the same chemical type, and coordination is possible in either a *cis* or a *trans* configuration, the difficulty arises that the ideal N–M–N angle may be, for example, 90° for *cis* donor atoms but 180° for *trans* donor atoms. The approach we adopted to overcome this difficulty was to alter the program to make the ideal angle a multiple of θ° and to allow the program to set the ideal value to be the nearest multiple of θ° to the trial value. With the use of appropriate angle bending parameters (vide infra) for the N–$\hat{M}$–N angles, this modification enabled us to model the domed Pb(II) porphyrin structure. The other metalloporphyrins required no special angle bending parameters, and the deformation force constants for N–M–N angles were set to zero.

Other minor, but nevertheless useful, modifications to the program involve menu-driven options concerning direction of output to monitor, file, or printer and the production of an output disk file directly importable into ALCHEMY II for easy plotting of the energy-minimized molecular structure. A listing of the changes made to MM2(87) is available as supplementary material. After alteration and compilation as outlined above, we verified the satisfactory performance of the modified program using test data for *trans*-cyclooctene provided by QCPE for the unmodified VAX version of MM2.

Parametrization of MM2(87) for Metalloporphyrins. The modeling of metalloporphyrin molecules by any currently available molecular mechanics packages involves the use of parameters over and above those available in their internal parametrization. At present such additional parameters are determined by a trial-and-error process aimed at reproducing molecular structures that are known from X-ray crystallographic studies. In this study, the structures of six metalloporphyrins, viz. the phosphorus(V),[45] planar and ruffled low-spin ($S = 0$) nickel(II),[39,40] zinc(II),[48] lead(II),[50] and intermediate-spin ($S = 1$) iron(II),[41] metalloporphyrins were used for purposes of parametrization. In addition, the

(93) Hancock, R. D. *Prog. Inorg. Chem.* **1989**, *37*, 188.
(94) Safo, M. K.; Gupta, G. P.; Walker, F. A.; Scheidt, W. R. *J. Am. Chem. Soc.* **1991**, *113*, 5497.
(95) Little, R. G.; Dymock, K. R.; Ibers, J. A. *J. Am. Chem. Soc.* **1975**, *97*, 4532.
(96) Higgins, T. B.; Safo, M. K.; Scheidt, W. R. *Inorg. Chim. Acta* **1990**, *178*, 261.
(97) Scheidt, W. R.; Osvath, S. R.; Lee, Y. J. *J. Am. Chem. Soc.* **1987**, *109*, 1958.
(98) Quinn, R.; Valentine, J. S.; Byrn, M. P.; Strouse, C. E. *J. Am. Chem. Soc.* **1987**, *109*, 3301.
(99) Hatano, K.; Safo, M. K.; Walker, F. A.; Scheidt, W. R. *Inorg. Chem.* **1991**, *30*, 1643.

(100) ALCHEMY II program: Tripos Associates, 6548 Clayton Road, St. Louis, MO.

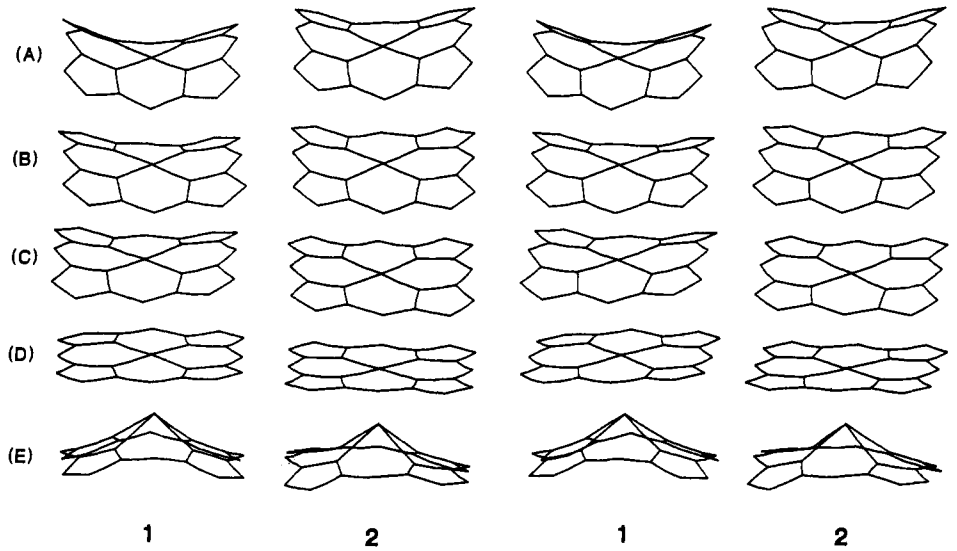

Figure 3. Comparative stereoview of (1) crystallographic and (2) molecular mechanics energy-minimized metalloporphyrin structures showing how the porphyrin core geometry depends on the metal ion size. The metal ions in the crystallographic structures and the mean $M-N_{porph}$ bond lengths are (A) P(V),[45] 1.891 Å; (B) (S = 0) Ni(II),[39] 1.929 Å; (C) (S = 1) Fe(II),[41] 1.971 Å; (D) Zn(II),[48] 2.026 Å; and (E) Pb(II),[50] 2.367 Å.

Table I. MM2(87) Atom Types Used in This Study

MM2 atom type no.	atom type	uses
1	sp^3 C	used for alkyl substituents
2	sp^2 C	used for porphyrin skeleton
5	H	used generally
37	N (−N=) azo, imi, pyrdine	used for axially coordinated imidazole nitrogen
40	sp^2 N pyrrole	used for porphyrin skeleton and noncoordinated imidazole nitrogens of axial ligands
49	sp^2 C	phenyl attached to porphyrin in TPP complexes
50	M	represents P(V), low-spin Ni(II), Zn(II), four-coordinate (S = 1) Fe(II), five- and six-coordinate high- and low-spin Fe(II/III), Pb(II)[a]

[a] Atom type number 50 was used generally for all metal ions, with the identity of the metal controlled with appropriate values of the equilibrium bond length (l_0) and stretching constant (k_s), appropriate torsional constants (for P(V) and Pb(II)), and angle bending constants (for Pb(II)).

crystal structures of ten imidazole complexes of Fe^{3+} porphyrins[46,47,94-99] were used for developing parameters for LS Fe^{3+}, while X-ray crystallographic data for HS and LS Fe^{2+} porphyrins were obtained from a review.[35] All parametrizations involved statistical comparisons of refined structures with crystal structures using the program COMPALL[101] as a standard procedure.

The MM2 atom types used in this study are listed in Table I. All atom type numbers ≤40 represent atom types that are fully parametrized in the MM2 program, and where they are concerned, the parameters used are those built into the program. Atom type numbers 49 and 50 represent new atoms for which torsional, stretching, dipole, van der Waals, angle bending, and "out-of-plane" angle bending parameters had to be developed. Numerical values for the additional parameters required for the metalloporphyrins investigated in this work are given in Table II.

The Effect of Metal Ion Size on Metalloporphyrin Core Geometry. With the exception of $[P(TPP)(OH)_2]OH$,[45] the crystal structures of the S_4-ruffled metalloporphyrins modeled were all 4-coordinate with a range of peripheral substituents. There appears to be little crystallographic evidence[37] to indicate that, other than the possible impact of phenyl group orientations on *sad* core conformations, peripheral substituents (where there is only modest steric crowding[19]) play anything but a minor role in determining the observed geometry of the porphyrin core. Thus, S_4-ruffled conformations are not unique to a specific type of porophinato ligand and may be found in complexes of OEP, TPP, and PPIX,[37] indicating that factors other than peripheral substituent effects are of importance here. The calculations relating to metal ion size therefore refer to 4-coordinate $[M(porphine)]^{n+}$ complexes with hydrogen atoms as peripheral substituents only. The hydroxide ligands of the S_4-ruffled $[P(TPP)(OH)_2]^+$ complex do not interact significantly with the porphyrin macrocycle and were removed.

We attempted to reproduce the degree of S_4 ruffling of the porphyrin cores shown in Figure 3 by changes in the unstrained metal-to-nitrogen bond lengths (l_o) and stretching constants (k_s), with all other parameters held constant. While this approach worked satisfactorily for metal ions of intermediate size (i.e., (S = 0) Ni(II), (S = 1) Fe(II) and Zn(II)), for very small (P(V)) and very large (Pb(II)) ions the extent of core ruffling could not be accurately simulated using this single parameter; suitable fits were only possible after modification of the torsional parameters involving the metal ion for both Pb(II) and P(V) (Table IIA) and, in addition, the N–M–N angle bending parameter for Pb(II) (Table IIE).

The best-fit size of a metal ion in a planar (D_{4h}) porphyrin core was investigated as follows. Available crystallographic data for a variety of metalloporphyrins indicate that planar core conformations occur with M–N bond lengths between 1.96 and 2.08 Å.[35] The values of l_o were varied between these limits with k_s = 5 mdyn/Å and all other values held constant. The total strain energy, U_T, was then plotted as a function of the energy-minimized M–N bond length to determine the bond length corresponding to the energy minimum.

Investigating the *sad* and *ruf* Forms of a Metalloporphyrin. The effect, principally on the strain energy of the core, of the progressive deformation of an initially planar $[Fe(porphine)]^+$ core to *ruf* and *sad* conformations was calculated as follows.

The distortion of the planar core of $[Fe(porphine)(2\text{-}MeIm)_2]^+$ to a *ruf* conformation was induced by progressively shortening the $Fe-N_{axial}$ bonds to the two axial 2-methylimidazole ligands (oriented with mutually perpendicular planes, such that each ligand plane bisected a *cis* N–Fe–N angle within the porphyrin core) from 2.40 to 1.70 Å. The $Fe-N_{axial}$ bond lengths and $N_{axial}-Fe-N_{axial}$ angle (180°) were fixed by restricting the positions of the three atoms prior to energy minimization of the structure. The axial ligands were subsequently removed and the strain energy of the refined core determined by restricting all core heavy atoms to their energy-minimized coordinates in the ruffled conformer, obtained in the presence of the axial ligands, and allowing only hydrogen atom positions to refine. The torsional parameters controlling the torsional angles around the $Fe-N_{axial}$ bond, where N is the donor nitrogen of an axially-coordinated imidazole group, were set to zero. This approach gave a satisfactory account of their orientations, which, particularly in the case of 2-methylimidazole, appeared to be controlled by steric interaction with the porphyrin core.

Increasing extents of *sad* ruffling of an initially planar $[Fe(TPP)]^+$ core were attained by counterrotation of an opposite pair of phenyl groups between dihedral angles of 90° and 30° to the porphyrin and allowing energy minimization of each structure. (The restricted dihedral angle defining the phenyl group orientation provides the driving force for *sad*

(101) COMPALL, program to statistically compare MM refined structures with crystal structures: Wade, P. W., 1991, Department of Chemistry, University of the Witwatersrand, P.O. WITS 2050, Johannesburg, South Africa.

Table II. Additional Parameters Used in MM2(87) for Modeling Metalloporphyrins

(A) Torsional Parameters (kcal·mol^{-1})[a]

atom I1	atom I2	atom I3	atom I4	V1	V2	V3	atom I1	atom I2	atom I3	atom I4	V1	V2	V3
5	49	49	5	0.0000	10.0000	0.0000	50	37	2	1	0.0000	10.0000	0.0000
5	49	49	49	0.0000	6.0000	−1.0600	50	37	2	2	0.0000	10.0000	0.0000
40	2	2	49	0.0000	5.4000	0.0000	50	37	2	5	0.0000	10.0000	0.0000
2	2	49	49	0.0000	0.0000	0.0000	37	50	37	2	0.0000	0.0000	0.0000
2	2	2	49	0.0000	10.0000	0.0000	2	2	40	50[b]	0.0000	1.5700	0.0000
2	49	49	49	−0.2700	10.0000	0.0000	2	2	40	50[c]	0.0000	16.0000	0.0000
2	49	49	5	0.0000	9.0000	−1.0600	2	40	50	40[b]	0.1000	−0.2000	0.1000
40	50	37	2	0.0000	0.0000	0.0000	2	40	50	40[d]	0.1000	−6.0000	0.1000
2	40	50	37	0.0000	0.0000	0.0000	40	2	2	1	0.0000	0.0000	0.0000
50	37	2	40	0.0000	10.0000	0.0000							

(B) Bond Stretching Parameters[e]

atom I	atom K	stretching constant, mdyn·Å^{-1}	min energy bond length, Å	atom I	atom K	stretching constant, mdyn·Å^{-1}	min energy bond length, Å	atom I	atom K	stretching constant, mdyn·Å^{-1}	min energy bond length, Å
40	50:LS Fe(III)	2.6800	1.9520	40	50:LS Ni(II)	2.5000	1.8910	37	50[f]	1.7000	1.9470
40	50:P(V)	5.0000	1.9440	40	50:IS Fe(II)	2.4000	1.9550	49	49	8.0670	1.3847
40	50:Pb(II)	2.5000	2.3620	40	50:HS Fe(II)	2.6800	2.0850	5	49	4.6000	1.1010
40	50:Zn(II)	1.8000	2.0200	40	50:LS Fe(II)	2.6800	1.9900	2	49	9.8000	1.4800
								1	49	4.4000	1.4870

(C) Bond Dipole Parameters[e]

atom I	atom K	bond moment, D	atom I	atom K	bond moment, D
40	50	0.0000	2	49	0.0000
37	50	0.0000	1	49	0.0000
49	49	0.0000			

(D) van der Waals Parameters

atom I	ϵ, kcal·mol^{-1}	r, Å
49	0.0440	1.9400
50	0.3838	1.2000

(E) Angle Bending Parameters[g]

atom I1	atom I2	atom I3	bending constant, mdyn·Å·rad^{-2}	min energy bond angle, deg	atom I1	atom I2	atom I3	bending constant, mdyn·Å·rad^{-2}	min energy bond angle, deg
2	2	49	0.4300	120.0	37	50	40	0.0000	90.0
2	49	49	0.4300	120.0	37	50	37	0.2800	180.0
49	49	49	0.4300	120.0	50	37	2	0.3000	125.0
5	49	49	0.3600	120.0	2	40	50	0.9000	125.0
40	50	40[h]	0.0000	90.0	2	40	2	0.4300	105.0
40	50	40[c]	0.0500	60.0	2	2	40	0.4300	108.0

(F) Out-of-Plane Angle Bending Parameters[i]

atom I2	atom I3	bending constant, mdyn·Å·rad^{-2}	atom I2	atom I3	bending constant, mdyn·Å·rad^{-2}
40	50	0.0500	49	49	0.0500
40	2	0.0500	2	49	0.0500
37	50	0.0500	5	49	0.0500

[a] Values refer to the dihedral angle I1–I2–I3–I4. V1, V2, and V3 are 1-fold, 2-fold, and 3-fold torsional constants, respectively. [b] For all metal ions except Pb(II) and P(V). [c] For Pb(II). [d] For P(V). [e] Values refer to the bond I–K. [f] For low-spin Fe^{3+}. [g] Values Refer to the Bond Angle I1–I2–I3. [h] For all metal ions except Pb(II). [i] Values refer to the situations in which atom I2 is out-of-plane relative to the attached atoms.

ruffling.) All four phenyl substituents were removed and replaced with hydrogen atoms, the heavy atoms were restricted, and the core strain energy was calculated as before.[102] The phenyl substituents were not treated as part of the same delocalized system as the core for the purpose of the SCF calculations on the π-electron system; if they were, the C–C torsional constants between the porphyrin core and phenyl substituents were found to be too large. It was therefore necessary to redefine the carbon atoms of the phenyl ring (atom type 49 in Table II) and to use standard[55] parameters to describe the phenyl rings. Since in unstrained structures there is a near perpendicular orientation between the phenyl rings and the porphyrin core, the torsional parameters between the sp^2 carbon atoms of the core and the phenyl groups were set to zero; the orientations of the phenyl groups were therefore controlled entirely by van der Waals interactions with the core. Bond and torsional angles were measured using ALCHEMY II; atomic deviations from the mean plane of the metalloporphyrin core were determined using XANADU.[103]

Results and Discussion

Porphyrin Core Geometry and Metal Ion Size. Figure 3 shows how the size of the metal ion coordinated by the porphinato macrocycle is a significant factor in determining the core conformation. Thus the P(V) complex is severely S_4 ruffled; the complexes of (S = 0) Ni(II) are either ruffled or planar; (S = 1) Fe(II) is moderately ruffled; Zn(II) is planar; and Pb(II) is C_{2v} domed. The ruffling of the porphyrin core may be quantified by measuring the C_m–M–C_m angle (Figure 2). By varying the M–N bond-stretching parameters (l_o and k_s) the structures of the planar and moderately ruffled porphyrins could be satisfactorily reproduced (Figure 3 and Table III). However, an accurate simulation of the core conformation of the severely ruffled P(V)

(102) The strain energy of the *core* is factored out as a component of the total strain energy of the complex with this method. Heavy atom constraints are required to preserve the core conformation obtained at each stage of the ruffling process so that the core strain energy can be calculated. Since the added H-atom coordinates are those calculated by ALCHEMY, they must be refined to obtain the correct core energy.

(103) XANADU, program for manipulation of crystallographic data: Roberts, P.; Sheldrick, G. M. 1976/7, private communication.

Table III. Ruffling Angles for Metalloporphyrins both Calculated Using MM2(87) and Observed in Crystal Structures[a]

M in $[M(porph)]^{n+}$	ruffling angle, deg	
	calcd[b,c]	obsd[c,d]
P(V)	154.9 (3.5)	151.1 (5.9)
Ni(II) (S = 0; S_4 ruffled)	167.7 (1)	162.4 (0)
Ni(II) (S = 0, planar)	179.8 (2)	180.0 (0)
Fe(II) (S = 1)	172.5 (4)	166.5 (0)
Zn(II)	179.1 (0)	179.5 (1)
Pb(II)	134.7 (5)	136.3 (6.6)

[a] The ruffling angle is the angle C_m–M–C_m indicated in Figure 2. [b] The calculated ruffling angles are for the porphyrin cores only with hydrogens as substituents on the periphery of the porphyrin ring. [c] The mean of the two ruffling angles is quoted, with a standard deviation computed as $\sigma_x = ([\sum x^2 - n\bar{x}^2]/n)^{1/2}$. [d] The observed ruffling angles are from a variety of metalloporphyrins: $[P(TPP)(OH)_2]^+$;[45] S_4-ruffled [Ni(OEP)];[39] planar [Ni(OEP)];[40] [Fe(TPP)];[41] [Zn(TPP)];[48] [Pb(T-PrP)].[50]

structure could only be achieved by increasing l_0 to resist overcompression of the M–N bonds (to bond lengths <1.80 Å), because S_4 ruffling of the core leads to a considerable radial contraction in the macrocycle cavity.[36,37] We found that the use of a negative 2-fold torsional constant, V2, for the C_a–N_j–P–N_{j+1} dihedral angles (j = 1, 2, 3; see Figure 2 for atom numbering), which change from the coplanar values of 0° and 180° as S_4 ruffling progresses, was necessary to provide the core with sufficient flexibility to simulate the rather extreme ruffling of the P(V) porphyrin. In the case of Pb(II), the N–M–N equilibrium bond angle had to be changed to 60° to accommodate the square-pyramidal coordination geometry of the metal ion, and a large, positive V2 torsional term for the C_b–C_a–N_{porph}–Pb and C_m–C_a–N_{porph}–Pb dihedral angles, which remain strictly close to 0° and 180°, respectively, as C_{2v} doming becomes more pronounced, was found necessary to cause the porphyrin core to dome toward the metal ion in the manner observed in the crystal structure of the complex. Clearly the very small size of P(V) on the one hand and the very large size of Pb(II) on the other placed additional requirements on the generalized force field we attempted to develop to reproduce metalloporphyrin structures. Table IV lists the root-mean-square differences between the MM2-predicted and crystallographically observed bond lengths, bond angles, and torsion angles. Representative data comparing calculated and observed bond lengths, bond angles, and torsion angles are available as supplementary material. As seen in Figure 4 for the core of $[P(TPP)(OH)_2]^+$,[45] bond lengths and angles are reasonably well predicted. It should be emphasized that all the parameters involving the porphyrin itself are unaltered from those in the MM2(87) program, and only the parameters involving the metal ion vary from one metalloporphyrin to the next. The differences in C–C bond lengths between the calculated and observed structure (Figure 4) of the $[P(porphine)]^{3+}$ core (and others) arise principally from the current application of the standard, simple heterocycle force constants in MM2(87) and the SCF MO treatment of less complex π-systems to the macrocyclic tetrapyrrole system of the metalloporphyrins.

The ruffling angles listed in Table III show that the energy-minimized geometries of the metalloporphyrin cores are in acceptable agreement with those of the crystal structures. Although

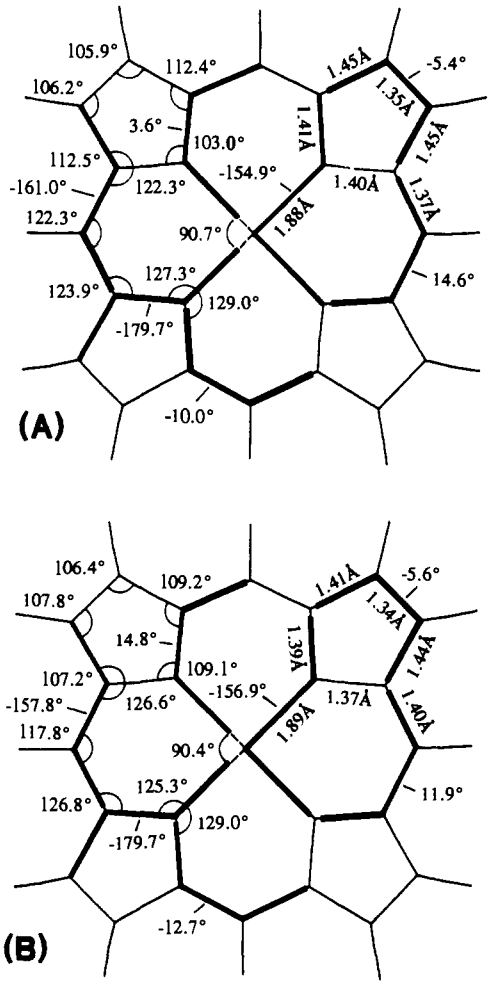

Figure 4. Details of bond lengths, bond angles, and torsional angles for P(V) porphyrins (A) as calculated using our current, modified MM2(87) force field for $[P(porphine)]^{3+}$ and (B) as observed[45] in $[P(TPP)(OH)_2]OH$. For simplicity and comparison, the phenyl groups and hydroxide ligands have been removed from the latter complex. The three bonds involved in each torsion angle are shown in heavy lines and the torsion angle is indicated at the central bond.

the number of structures investigated is small, it appears that with the exception of very small and very large metal ions the force constants incorporated in MM2(87) together with l_0 and k_s values for the M–N bonds are capable of predicting the structures of metalloporphyrins reasonably well. For very large and very small metal ions considerably less pliant torsional and/or angle bending constants had to be used to accommodate the very severe distortion of the core.

Provided the parameters for Zn(II) were used, this planar structure could be obtained even when starting from highly distorted trial structures such as those observed for the P(V) and Pb(II) porphyrins; this was taken to be an indication of the reliability of the minimizer in locating true minima in conformational space. The present calculations therefore suggest that the size

Table IV. Root-Mean-Square Differences between Crystal and MM2-Predicted Structures of the Porphyrins[a,b]

		Ni(porph)				
	$P(porph)^{3+}$	ruffled	planar	Fe(porph)	Zn(porph)	Pb(porph)
bonds (M–N)	0.018	0.001	0.017	0.005	0.002	0.004
bonds (porph)	0.047	0.045	0.039	0.034	0.030	0.035
angles (M–N–M)	1.8	0.5	0.2	0.6	0.7	2.2
angles (M–N–C)	2.5	1.4	1.2	1.3	1.1	2.4
angles (porph)	3.1	1.8	1.3	1.6	1.3	1.1
torsions (M–N)	6.3	6.0	1.1	6.2	4.8	8.4
torsions (porph)	4.1	4.1	1.1	4.9	4.4	9.9

[a] A listing of selected calculated and observed bond lengths, bond angles, and torsional angles is available as supplementary material. [b] Bonds in Å, angles in deg, and atomic displacements in Å.

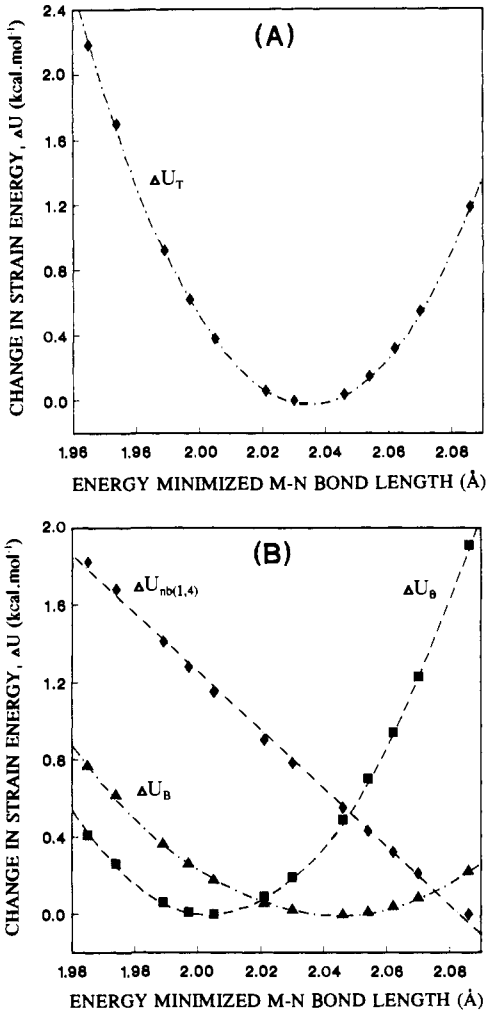

Figure 5. (A) Plot of the change in total strain energy (U_T) as a function of the energy-minimized M–N bond length for the planar conformer of a D_{4h} [M(porphine)]$^{n+}$ complex. The curve was generated by fixing k_s at 5.00 mdyn/Å and varying l_o from 1.95 to 2.10 Å. The turning point at 2.035 Å represents the minimum-strain M–N bond length. (B) Plot of the significant contributions to U_T made by bond length deformation (U_B), bond angle deformation (U_θ), and [1,4] van der Waals interactions ($U_{nb(1,4)}$) as a function of the energy minimized M–N bond length.

of Zn(II) is such that a planar porphyrin structure is always favored. When investigating ruffled porphyrins it was found that if the trial structure is exactly planar then the program may not generate an appropriately S_4-ruffled core conformation (with small metal ions) but may converge to a local minimum, either with a totally planar porphyrin or one showing ruffling of non-S_4 symmetry (usually twisted). To investigate the *extent* of S_4 ruffling, therefore, requires starting with an appropriate, mildly-S_4-ruffled trial structure.

The force field developed may be used to calculate the total strain energy of a metalloporphyrin as a function of metal ion size. This was done for a planar (D_{4h}) porphyrin. In this type of calculation all parameters in the force field are kept constant except for the strain-free M–N bond length[68] which was varied between 1.950 and 2.100 Å. The strength of the parameters involving the metal ion will affect the steepness of the curve but has virtually no effect on the position of the minimum in the curve,[68] particularly when the macrocycle retains conformational symmetry as the value of l_o is varied between the required limits.[104] The dependence of the total strain energy on the energy-minimized M–N bond length is shown in Figure 5A. It was found that the torsional strain energy did not change with M–N bond length;

Table V. Steric Energy Components (kcal·mol^{-1}) and Structural Parameters in the MM Energy-Minimized Planar and Ruffled Forms of (S = 0) [Ni(porphine)] and (S = 1) [Fe(porphine)]

	[Ni(porphine)]		[Fe(porphine)]	
	planar	S_4 ruffled	planar	S_4 ruffled
Steric Strain Components				
bond length deformation	2.40	1.54	0.86	0.75
angle bending	43.28	42.15	42.36	42.26
stretch-bend	0.74	0.55	0.32	0.25
van der Waals				
[1,4]	2.92	2.77	2.24	2.22
other	−3.42	−3.52	−3.38	−3.42
torsion	−19.07	−15.18	−19.84	−18.53
dipole	0.54	0.54	0.51	0.51
total	27.39	28.86	23.08	24.04
Structural Parameters				
M–N, Å				
predicted	1.942	1.929	1.980	1.973
observed	1.957[a]	1.929[b]		1.972[c]
∠C_m–M–C_m, deg				
predicted	179.8	167.7	180.0	172.5
observed	180.0[a]	162.4[b]		166.5[c]

[a] Reference 40. [b] Reference 39. [c] Reference 41.

this is as expected since the porphyrin conformation investigated was perfectly planar. Dipole, stretch-bend, and nonbonded (other than [1,4] interactions) strain energies did not change significantly. The main contributors to the energy dependence of Figure 5A are the [1,4] nonbonded van der Waals interactions, bond length deformations, and bond angle deformations (Figure 5B). The curve of Figure 5A is parabolic and has a turning point at 2.035 Å, in agreement with the suggestion that the ideal M–N bond length for coordination in the porphyrin ring is 2.01–2.04 Å.[36,105] At longer M–N bond lengths, U_T increases principally due to an increase in bond angle deformations; at shorter M–N bond lengths the increase in U_T is due predominantly to increases in nonbonded interactions but bond compression and bond angle deformation play a role as well (Figure 5B).

The Planar and Ruffled Forms of (S = 0) Ni(II) and (S = 1) Fe(II) Porphyrins. Both planar and ruffled forms of (S = 0) [Ni(OEP)] exist in solution[20] and in the solid state;[39,40] only the S_4-ruffled conformation of (S = 1) [Fe(TPP)] has been reported in the solid state.[41] Using MM calculations we have found that both planar and ruffled cores of Ni and Fe porphyrins are attainable (Table V). With a planar or severely ruffled (P(V) core) porphyrin as trial structure the planar energy-minimized structures are obtained, whereas starting with the S_4-ruffled crystal structures allows location of local minimum conformations that have largely retained the extent of ruffling present in the crystal structures. In both cases the planar conformation is marginally more stable (by 1–1.5 kcal·mol^{-1}). This suggests that the S_4-ruffled conformation of these two metalloporphyrins observed in the crystalline solid state corresponds to a higher energy conformer of an energetically favored planar D_{4h} species in solution. More specifically, having demonstrated that the S_4-ruffled conformation of the [Ni(porphine)] core of [Ni(OEP)] is less stable than the planar conformation and that the energy difference is small, it becomes possible to rationalize the observation that both forms coexist in solution[20] in terms of their relative energies. Further, the ruffled conformation of [Ni(OEP)] has a lower packing energy in the solid state[40] and the same may well hold for [Fe(TPP)] so that, despite its greater (predicted) solution state stability, the solid-state planar conformation has not yet been observed.

The Extrusion of Iron from the Porphyrin Macrocycle on Change of Spin State. An important aspect of Perutz's cooperativity model[106] for the loading of O_2 by hemoglobin entails the rising of Fe(II) out of the mean porphyrin plane on deoxygenation. This structural change could be dictated either by (i) the metal ion attempting to escape the steric compression consequent on the

(104) Drew, M. G. B.; Yates, P. C. *J. Chem. Soc., Dalton Trans* **1986**, 2506.

(105) Fleisher, E. B. *Acc. Chem. Res.* **1970**, *3*, 105.
(106) Perutz, M. F. *Proc. R. Soc. London, Ser. B* **1969**, *173*, 113.

Table VI. Structural Parameters and Strain Energies of Energy-Optimized Four-Coordinate Fe(II) Porphyrins

	energy-minimized structures of [Fe(porphine)]		
	planar HS	domed HS	planar LS
l_0, Å	2.085	2.085	1.990
k_s, mdyn·Å^{-1}	2.68	2.68	2.68
strain energy, kcal·mol^{-1}			
U_T	23.10	21.79	21.92
U_θ	43.73	42.85	42.21
U_ϕ	−19.10	−19.62	−19.87
U_B	0.42	0.15	0.35
porphyrin cavity diameter (N_1–N_3), Å	4.156 (1)	4.103 (1)	4.005 (0)
Fe–Ct_p, Å	0.003	0.32	0.009
$\angle C_m$–Fe–C_m, deg	179.9	169.3	179.7
$\angle N_1$–Fe–N_3, deg	180.0	163.0	179.5
$\angle N_1$–Fe–N_2, deg	90.0	88.8	90.1
Fe–N_{porph}, Å	2.078	2.074	2.003
C_{av}, Å	0.003	1.070	0.010

increase in its ionic radius accompanying the change in its spin state or (ii) the dictates of the ion's coordination chemistry with a five- and six-coordinate complex expected to have the ion above, and in, the porphyrin ring, respectively, to optimize bonding to the axial ligands.

To determine the importance of steric factors in the absence of axial ligands, a four-coordinate [Fe(porphine)] complex was used as a model. With high-spin Fe(II), the starting planar structure with a core cavity (N_1–N_3) of 3.985 Å refined (Table VI) to a planar structure (with iron displaced from the mean plane of the four pyrrole nitrogens, Fe–Ct_p = 0.003 Å) with an expanded porphyrin core (4.156 Å). When the starting structure was changed to one with the metal ion slightly displaced (0.07 Å) above the planar porphyrin, the structure underwent C_{2v} doming (where the metalloporphyrin core exhibits a folding axis along the direction of the N_2–Fe–N_4 vector and has pyrrole rings 2 and 4 approximately in the mean porphyrin plane, with rings 1 and 3 tilted to the same extent below this plane) with Fe(II) 0.32 Å above the mean plane and a smaller expansion in the core cavity (4.103 Å). Starting with this domed structure or the planar structure and changing the parameters of the metal to those appropriate for low-spin Fe(II) led to an optimized planar structure with a core cavity of 4.005 Å.

The domed HS structure is more stable than the planar HS structure by a very modest 1.3 kcal·mol^{-1}, due principally to a decrease in angle bending and torsional strain throughout the macrocycle. There is very little difference in energy between the domed HS structure and the planar LS structure.

These results emphasize the flexibility of the porphyrin ring, accommodating, in the two planar structures, an expansion of the core cavity of 0.15 Å at the expense of 1.3 kcal·mol^{-1}. The larger ionic radius of HS Fe(II) can, without a significant energy penalty,

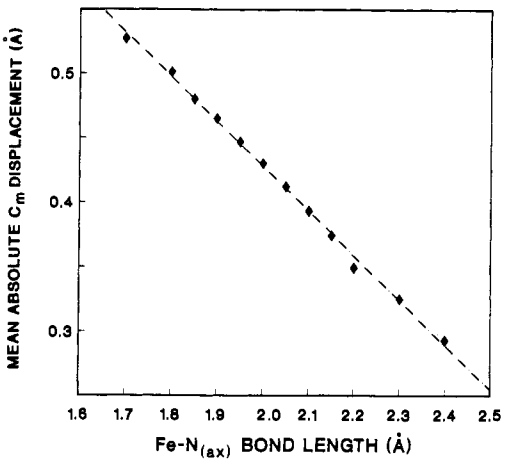

Figure 6. Plot of the variation in the extent of *ruf* ruffling of an [Fe(porphine)]$^+$ core, as measured by the mean absolute perpendicular displacement of the methine carbons (C_m), as a function of the bond length [Fe–$N_{(ax)}$] to 2-methylimidazole in the complex [Fe(porphine)-(2-MeIm)$_2$]$^+$, with the planes of the 2-MeIm groups bisecting the N–Fe–N angles of the core and oriented at 90° to each other.

be accommodated quite adequately by an expansion of the porphyrin core and does not require an extrusion of the metal ion from the macrocyclic cavity. Generally, HS 5-coordinate Fe(II) porphyrins such as deoxyMb are observed with Fe(II) about 0.4 Å above the mean porphyrin plane; even in 5-coordinate LS complexes such as [Fe(TPP)(NO)][35] the metal ion is found 0.22 Å above the mean plane. In 6-coordinate complexes, however, whether HS or LS, the metal is either in or very close to the mean plane.[35] We may therefore tentatively conclude that steric compression does not play a dominant role in determining the position of Fe(II) in ferrous porphyrins and that the dominant effect appears to be the dictates of its favored coordination geometry. Further aspects of this are currently under investigation and will be reported on elsewhere.

The Occurrence of *sad* and *ruf* Forms of Metalloporphyrins. There are available planar,[97] *ruf*,[46,47] and *sad*[96,107] forms of Fe(III) TPP six-coordinate complexes with axially coordinated imidazoles. Depending on the relative orientation of two axial 2-methylimidazole groups, the porphyrin core can be present with either a planar[97] or *ruf*[46] geometry. The present MM calculations show (and X-ray structures support this[46,47]) that *trans* axial imidazole ligands whose planes are approximately perpendicular to each other, and bisect the *cis* N–Fe–N angles of the metalloporphyrin core, induce a *ruf* conformational geometry. Table VII and Figure 6 show how the extent of *ruf* ruffling is predicted to vary with the length of the M–N_{axial} bond of the coordinated imidazoles. As the imidazole ligands are pulled in toward the core, so the amount of ruffling is increased by the van der Waals contacts between them and the surface of the porphyrin core in the region

Table VII. Variation in Intrinsic Core Strain Energy and the More Important Strain Energy Components (kcal·mol^{-1}), and Conformational Geometry, as a Function of Increased S_4 Ruffling Caused by Shortening of the Fe–N Bond to the Axial 2-Methylimidazole Ligands of [Fe(porphine)(2-MeIm)$_2$]$^+$ [a]

Fe–$N_{(ax)}$ [b]	C_m [c]	C_{av} [d]	intrinsic core strain energy [e]	U_B	U_θ	U_{NB} [1,4]	U_{NB}	U_ϕ
2.40	0.29	0.16	24.97	0.66	42.02	−3.45	2.23	−17.09
2.30	0.33	0.18	25.07	0.55	41.84	−3.46	2.18	−16.65
2.20	0.35	0.20	24.52	0.52	41.69	−3.47	2.12	−16.94
2.10	0.39	0.22	25.52	0.42	41.44	−3.49	2.05	−15.51
2.00	0.43	0.24	25.84	0.36	41.22	−3.51	1.98	−14.81
1.90	0.47	0.26	26.19	0.30	41.01	−3.52	1.91	−14.12
1.80	0.50	0.28	26.71	0.25	40.88	−3.54	1.84	−13.33
1.70	0.53	0.30	26.97	0.24	40.63	−3.56	1.75	−12.72

[a] Calculated for the porphine complex of Fe(III), where porphine is the porphyrin core with only hydrogens as peripheral substituents. [b] The Fe–$N_{(ax)}$ bond lengths (Å) to the *trans*-2-MeIm ligands were fixed during energy minimization by restriction of the $N_{(ax)}$–Fe–$N_{(ax)}$ atoms at an angle of 180° at the indicated distances. [c] C_m is the mean perpendicular displacement (Å) of the C_m carbon atoms (see Figure 2) from the mean plane of the metalloporphyrin. [d] C_{av} is the mean perpendicular displacement of the 25 non-hydrogen atoms from the mean plane of the [Fe(porphine)]$^+$ core. [e] The intrinsic strain energy (kcal·mol^{-1}) of the [Fe(porphine)]$^+$ core is calculated by refinement of the H-atom positions following removal of the axial ligands and restriction of the core heavy atoms to their energy-minimized coordinates.

Table VIII. Variation in Strain Energy, the More Important Strain Energy Components, and Conformation of the [Fe(porphine)]$^+$ Core as a Function of the Phenyl Dihedral Angles (Ph1 and Ph3) of [Fe(TPP)]$^+$

phenyl dihedral angle[a]	C_b[b]	C_{av}[c]	U (complex)[d]	core strain energy[e]	U_θ (core)[f]	U_ϕ (core)[g]	U_ϕ (complex)[h]
90.0	0.02	0.02	8.25	23.46	42.33	−19.76	−41.49
80.0	0.02	0.02	8.69	23.51	42.26	−19.78	−41.40
70.0	0.03	0.03	10.75	23.90	42.34	−19.41	−40.96
60.0	0.12	0.07	11.71	24.22	42.12	−18.84	−40.14
55.0	0.14	0.10	13.11	24.49	42.06	−18.51	−39.44
53.5	0.28	0.17	12.97	24.60	41.65	−17.85	−38.90
50.0	0.32	0.20	14.13	24.75	41.52	−17.48	−38.14
45.0	0.41	0.26	16.02	25.19	41.10	−16.45	−36.45
40.0	0.49	0.31	17.34	24.85	40.68	−16.23	−35.50
35.0	0.57	0.35	19.27	25.44	40.19	−14.99	−33.63
30.0	0.67	0.42	22.69	26.42	39.57	−13.13	−30.54

[a] Fixed dihedral angles (deg) for the phenyl groups attached to C_{m1} and C_{m3} on the porphyrin ring (see Figure 2). [b] Mean perpendicular displacements of the C_b carbons from the mean plane of the metalloporphyrin (Å). [c] Mean perpendicular displacements of non-hydrogen atoms from the mean plane of the metalloporphyrin (Å). [d] Total strain energy (kcal·mol^{-1}) of the complex [Fe(TPP)]$^+$. [e] Intrinsic strain energy (kcal·mol^{-1}) of the [Fe(porphine)]$^+$ core calculated, after replacement of the phenyl substituents with H atoms, by refinement of the hydrogen positions with the core heavy atoms restricted to their energy-minimized coordinates. [f] Angle bending energy in the core (kcal·mol^{-1}). [g] Torsion angle energy in the core (kcal·mol^{-1}). [h] Torsion angle energy (kcal mol^{-1}) in the complex [Fe(TPP)]$^+$.

of lines bisecting the N–Fe–N angles of the core.

Schedit and Lee[37] have demonstrated the preponderance of the *sad* core geometry in [M(TPP)]$^{n+}$ complexes. This conformation is always observed when one or more of the phenyl dihedral angles is <60°, presumably because such a conformational geometry most efficiently minimizes repulsive nonbonded interactions between the tilted phenyl substituents and the *b* CH groups of the porphyrin pyrrolic units. Two crystal structures of six-coordinate Fe(III) porphyrins with a *sad* conformation have been reported, namely [Fe(TPP)(1-MeIm)$_2$]ClO$_4$[96] and [Fe(TPP)(4-MeIm$^-$)$_2$]$^-$.[107] In both structures, the dihedral angles between the phenyl substituents and the porphyrin are small (<65°), and the available crystallographic evidence[37] suggests that intermolecular interactions between neighboring molecules (whether dimeric, aggregated, or merely close packed) in the solid state are probably responsible for the tilting of the phenyl substituents away from the normal to the porphyrin plane. It would appear that crystal packing forces that require the severe tilting of phenyl substituents override the conformational dictates of the orientation of the axial ligands and the *sad* rather than the *ruf* conformer becomes favorable as a means of minimizing nonbonded repulsive interactions between the phenyl substituents and the porphyrin ring.

This was investigated by counterrotating an opposite pair of phenyl substituents on an [Fe(TPP)]$^+$ core (Table VIII and Figure 7). The extent of *sad* ruffling (as measured by the mean perpendicular displacement of *b*-carbon atoms from the mean metalloporphyrin plane) increases nonlinearly as the dihedral angle is decreased to 30°. It may be noted that the smallest known phenyl dihedral angle in a TPP complex is 38.6°, in the [Cu(TPP)]$^+$ cation.[108] Significant *sad* ruffling of the porphyrin core (i.e., mean C_b displacement >0.15 Å) is only observed for dihedral angles <55°, where a distinct step in the extent of ruffling appears to occur (Figure 7). This probably reflects the critical dihedral angle below which minimization of intramolecular nonbonded contacts occurs by the porphyrin adopting a marked *sad* conformation. Figure 7 thus provides an explanation for the observation[37] that [M(TPP)]$^{n+}$ structures with one or more phenyl dihedral angles smaller than 55° exhibit *sad* core conformations. The total strain energy increases smoothly with decreasing phenyl dihedral angle (Figure 7) on account of the variation of the dominant torsional strain component as the phenyl groups are tipped toward the pyrrole rings and therefore propagate the rotational deformation of torsion angles within the metalloporphyrin core.

We have calculated the mean phenyl dihedral angle from the smallest observed dihedral angles in several *sad* [M(TPP)]$^{n+}$ complexes as reported by Scheidt et al.[37,96] and find that as the dihedral angle decreases so the mean absolute *b*-carbon displacements show a general linear increase (Table IX and Figure 8). The calculations consistently underestimate the mean observed

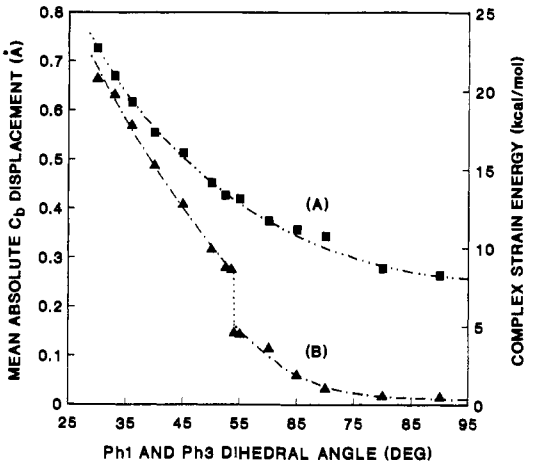

Figure 7. Plot of the variation of the total strain energy of the complex [Fe(TPP)]$^+$ (A) and the magnitude of the *sad* ruffling of its [Fe(porphine)]$^+$ core (B) as a function of the counterrotation of an opposite pair of phenyl substituents (Ph1 and Ph3) to the fixed values of the phenyl dihedral angle (relative to the plane of the metalloporphyrin core) shown. Buckling of the core into a *sad* geometry is measured by the mean absolute perpendicular displacement of the C_b carbons from the mean plane of the metalloporphyrin core.

Table IX. Variation in *sad* Core Geometries with Ph Dihedral Angles for Some M(TPP) Complexes[a]

complex	C_b, Å	mean of the smallest dihedral angles,[b] deg
[Fe(TPP-C$_5$Im)(THT)]	0.11 (4)	66.4 (1.6)
[Fe(TPP)]$_2$SO$_4$	0.14 (3)	64.4 (8)
[Zn(TPyP)(Py)]	0.15 (3)	62.0 (4.2)
[Mn(TPP)(4-MePip)(NO)]	0.16 (4)	65.9 (2.5)
[Fe(TPP)(4-MePip)(NO)]	0.16 (3)	67.3 (2.6)
[Mn(TPP)(1-MeIm)]	0.18 (7)	56.4
[Fe(TPP)(PMS)$_2$]ClO$_4$	0.18 (2)	63.6 (4)
[Fe(TPP)(4-MeIm$^-$)$_2$]	0.19 (3)	61.7 (3.3)
[Fe(TPP)(NO)(1-MeIm)]	0.22 (2)	60.7
[Fe(TPP)(1-MeIm)$_2$]ClO$_4$[c]	0.23 (5)	59.0 (4.1)
[Fe(TAP)(SH)]	0.25 (9)	56.2 (1.7)
[Co(TPP)(SC$_6$HF$_4$)$_2$]$^-$	0.28 (8)	62.0 (6.5)
[Mo(TPP)O]	0.32 (23)	59.0 (4.0)
[Cr(TPP)N]	0.35 (10)	52.5 (1.8)
[Mn(TPP)(NO)]	0.35 (10)	54.9 (4)
[Cr(TPP)O]	0.39 (9)	51.6 (1.0)

[a] Data from reference 37. [b] Dihedral angles <70°. [c] Reference 96.

(107) Quinn, R.; Strouse, C. E.; Valentine, J. S. *Inorg. Chem.* **1983**, *22*, 3934.
(108) Scholz, W. F.; Reed, C. A.; Lee, Y. J.; Scheidt, W. R.; Lang, G. *J. Am. Chem. Soc.* **1982**, *104*, 6791.

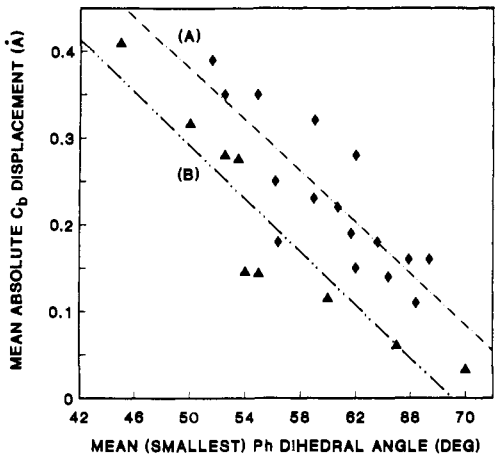

Figure 8. Plot of the trends in the extent of *sad* ruffling of $[M(TPP)]^{n+}$ cores as a function of the mean of the smallest phenyl dihedral angles in the complex. Data from a range of $[M(TPP)]^{n+}$ crystal structures with various ligands and metal ions (Table IX) have been plotted as the experimental points (♦) on relationship (A). The core geometries calculated (▲) using MM2 are obtained from Table VIII and plotted as relationship (B).

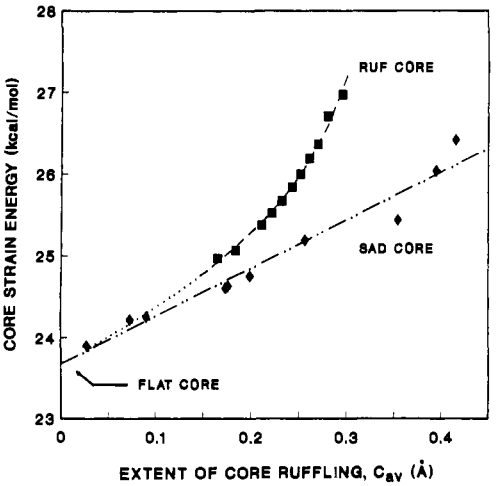

Figure 9. Plot of the intrinsic strain energies of $[Fe(porphine)]^+$ cores with *sad* and *ruf* geometries as a function of the extent of ruffling of the core, C_{av}, where C_{av} is the root-mean-square displacement of the 25 core heavy atoms from the mean plane of the metalloporphyrin core.

b-carbon displacement by about 0.08 Å. This may be due, in part, to the internal parametrization of MM2 and the SCF calculations performed on the π-system. MM2 appears to reproduce the *ruf* conformation in the presence of axial ligands more readily than the *sad* conformation, which is driven by the orientation of the phenyl substituents. It seems likely that the steric repulsion between the phenyl groups and the porphyrin core is only moderately well transmitted by the force field throughout the macrocycle.

The Relative Energies of the *sad* and *ruf* Forms of Ruffling. To be able to compare the intrinsic strain energies of two core conformations, a symmetry-independent measure of the extent of core distortion is needed. We have chosen to use the root-mean-square deviation (C_{av}[96]) of the 25 heavy atoms of the core from the mean plane they describe. The intrinsic strain energies of the *sad* and *ruf* $[Fe(porphine)]^+$ cores are plotted as a function of C_{av} in Figure 9. In Figure 10 the dominant strain energy components of the total strain energy are plotted as *changes* in strain energy with core conformation.

The *ruf* and *sad* cores show nonlinear and linear increases in strain energy, respectively, with increasing C_{av} (Figure 10). A linear decrease in angle-bending strain in conjunction with a steep, nonlinear increase in torsional strain for the *ruf* conformation results in an apparent exponential increase in the strain energy

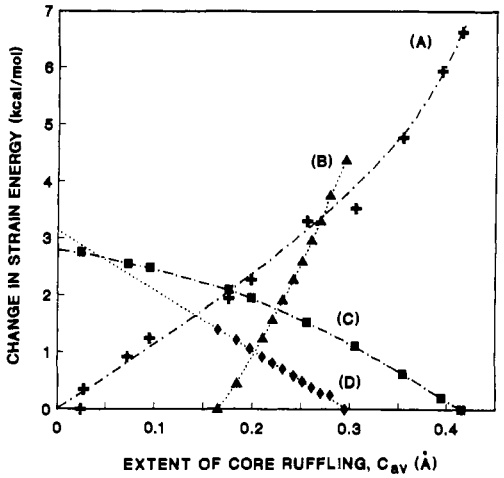

Figure 10. Plot of the change in strain energy with increasing nonplanarity of the core geometry, measured by C_{av}, for the major strain energy components of *ruf* and *sad* $[Fe(porphine)]^+$ core conformations. Lines (A) and (B) are the torsional components of the total strain energy for the *sad* and *ruf* cores, while lines (C) and (D) are the respective angle bending components of the total strain energy.

with increasing core buckling. In contrast, the angle-bending and torsional components of the strain energy for a *sad* conformation decrease and increase, respectivley, in an approximately linear fashion, leading to the apparent linear dependence shown in Figure 10. The other strain energy components show a small linear variation with the extent of core ruffling and contribute little to the total strain energy. The dominant factor contributing to an increase in the intrinsic strain energy with buckling of the core arises from torsions about $M-N_{porph}$ and C_a-C_m bonds in *ruf* cores, and in addition from torsions about C_a-C_b bonds in *sad* cores. It is therefore likely that for all metalloporphyrins relations analogous to those of Figure 10 for iron(III) porphyrins will arise.

The results presented in Figure 10 show that, at least for the $[Fe(porphine)]^+$ core, the planar conformation is more stable than the *ruf* or *sad* conformation. For a complex such as $[Fe(TPP)(2\text{-MeIm})_2]ClO_4$,[46] with a C_{av} value of 0.21 Å,[46,96] the energy difference between a planar and a *ruf* conformation is only 1.6 kcal·mol^{-1}. In general, *sad* and *ruf* conformations tend to have values of C_{av} in the range of 0.10–0.25 Å, for which only small energy differences between the planar, *sad*, and *ruf* geometries appear to exist (Figure 10). This suggests that, particularly in highly substituted metalloporphyrins,[19,52] core deformation is an efficient stereochemical pathway that allows for minimization of nonbonded interactions between substituents on the periphery of the porphyrin ring.

The Flexibility of the Porphyrin Core. The results obtained in the present work demonstrate that the metalloporphyrin core is flexible and that a considerable range of core conformations should be attainable for many metalloporphyrins. This is confirmed by the recently reported[20] resonance Raman studies where planar and ruffled conformers of nickel(II) porphyrins have been shown to coexist in solution and where unique nonplanar conformations may be promoted by π donor–acceptor complexes with planar aromatic guest molecules.[109]

Given the flexibility of the porphyrin core it is not surprising to find that interactions between the heme group(s) and side chains of amino acid residues in hemoproteins contribute appreciably to the observed geometry of the prosthetic group. Reference to some recently reported high-resolution (<1.8 Å) structures of hemoproteins will serve to illustrate this. In both oxidized[24] and reduced[25] tuna cytochrome *c*, the plane of the coordinated axial His-18 bisects the $N_{porph}-Fe-N_{porph}$ angle (47°), while the $S-C_\gamma$ bond of the *trans* Met-80 bisects the same angle in an adjacent quadrant; the $C_\alpha-C_\beta-C_\gamma$ chain of Met-80 lies over the C_a-C_m bond of a pyrrole ring. As predicted by the present work, and observed

(109) Alden, R. G.; Ondrias, M. R.; Shelnutt, J. A. *J. Am. Chem. Soc.* **1990**, *112*, 691.

in the cytochromes *c*,[24-28] such interactions cause the porphyrin to adopt a *ruf* core conformation. A nonbonded interaction between Arg-48 and one of the pyrrole rings of the heme group in cytochrome *c* peroxidase[29,30] causes the porphyrin ring to bend away from the amino acid side chain while a $\pi-\pi$ attractive interaction between the adjacent pyrrole ring and the Trp-51 residue promotes the saddling of the heme group in this enzyme.

Conclusions

We have shown, using the internal parameters of MM2(87) and newly-developed parameters for metal ions, that MM techniques can be used to accurately simulate the structure of metalloporphyrins containing a wide range of size of metal ion and hence extent of porphyrin core ruffling. The conformations of metalloporphyrin complexes were investigated as a function of metal ion size for a *porphine* ligand only, as conformational geometries were insensitive to peripheral substituent effects, in contrast to *sad* conformations of $[M(TPP)]^{n+}$ complexes.

For the ions Ni(II), Fe(II), and Zn(II) the extent of core ruffling could be satisfactorily reproduced by varying the M–N bond-stretching parameters. For very small P(V), specific torsional parameters involving the central ion had to be adjusted to induce the observed ruffling of the porphyrin core. For very large Pb(II), moreover, the N–M–N equilibrium bond angle had to be reduced from 90° to 60° to accommodate the observed square-pyramidal coordination geometry about the metal ion.

Using a planar (D_{4h}) metalloporphyrin core conformation, all parameters in the force field were kept constant while the M–N equilibrium bond length was varied. The variation in the total strain energy with this parameter showed that the best-fit size of metal ion in the porphyrin cavity is 2.035 Å. Strain energy increases for larger metal ions are principally due to bond angle deformation. Smaller metal ions cause an increase in the nonbonded van der Waals interactions; there is also some contribution to an increase in total strain energy from bond compression and bond angle deformation.

Low-spin ($S = 0$) [Ni(OEP)] is known to exist in solution and in the solid state as a planar and a ruffled structure. We have shown that there are compensating increases in torsional strain and decreases in bond length and bond angle deformation in going from a planar to a ruffled structure so that the energy difference between the two is very small (<1.5 kcal·mol^{-1}). Further, our calculations predict the existence of a planar form of intermediate spin ($S = 1$) [Fe(TPP)], the ($S = 1$) [Fe(porphine)] core of which is <1 kcal·mol^{-1} more stable than the experimentally observed ruffled form. It is possible that other metal ions, having radii within the range delimited by ($S = 0$) Ni(II) and ($S = 1$) Fe(II), may be of such a size that in the absence of axial ligands both ruffled and planar forms of the metalloporphyrin are attainable.

We have shown that steric factors alone do not explain why five-coordinate high-spin Fe(II) porphyrins have the metal ion above the mean porphyrin plane whereas in six-coordinate low-spin Fe(II) complexes the metal ion resides in the mean plane. At a very modest expense of 1.3 kcal·mol^{-1} (due principally to an increase in bond angle deformation) the porphyrin ring can undergo a core expansion of 0.15 Å to accommodate the increase of metal ion radius accompanying a change in spin state. It is therefore suggested that the extrusion of the metal ion from the mean plane of the four porphinato nitrogen donors is mainly dependent on the dictates of its favored coordination geometry. Thus, irrespective of the oxidation and spin state of the coordinated metal ion, and hence its radius, a 5-coordinate metalloporphyrin will display a square-pyramidal coordination geometry with the metal ion displaced from the mean porphyrin plane toward the axial ligand. Addition of a sixth ligand triggers conversion to an octahedral configuration with the metal ion lying in the plane of the four nitrogen donors, as this arrangement best minimizes intramolecular ligand–ligand interactions.

Two forms of ruffling (*sad* and *ruf*) are commonly observed with metalloporphyrins. A *ruf* conformation is shown to occur in six-coordinate Fe(III) porphyrins when two *trans* imidazole axial ligands with mutually perpendicular ligand planes bisect *cis* N–Fe–N angles in the porphyrin core, and the extent of ruffling is shown to increase monotonically as the Fe–N_{axial} bond length decreases. We have demonstrated that a *sad* conformation (usually found in $[M(TPP)]^{n+}$ complexes) arises from the tipping over of phenyl substituents of the TPP core, presumably in response to factors such as packing forces in the solid state. Our calculations show (and reference to available structures confirms) that the extent of *sad* ruffling is directly related to the dihedral angle between the porphyrin ring and the phenyl substituents and becomes considerable for dihedral angles <55°. Calculations on S_4 ruffling in $[Fe(porphine)(2\text{-MeIm})_2]^+$ complexes were performed with hydrogen atoms as peripheral substituents because preliminary work on $[Fe(TPP)(2\text{-MeIm})_2]^+$ complexes indicated that, on occasion, incomplete refinement of the core geometry of the complex occurred.[110] Variations in *core* strain energies for *sad* and *ruf* metalloporphyrin conformations were analyzed by factoring out this component from the total complex strain energy.

A planar core (at least for Fe(III) porphyrins) is always more stable than a *sad* or a *ruf* core, although the energy differences are small for the extent of ruffling usually observed in metalloporphyrins. Porphyrins are therefore capable of adopting a variety of conformations in response to such factors as the orientation of axial ligands and the interaction with their environment. This conclusion is verified by examining the nature and extent of porphyrin ruffling in the hemoproteins.

Acknowledgment. The authors thank Professor P. W. Linder and Mr. A. Voye of the University of Cape Town for valuable discussions on this work. The University of the Witwatersrand and the Foundation for Research Development are thanked for generous financial support for this work. AECI Ltd. is thanked for a postgraduate fellowship to O.Q.M. The Quantum Chemistry Program Exchange is thanked for providing a copy of the MM2(87) program.

Appendix. The MM2(87) Force Field Potential Function

The potential energy function used to calculate the total strain energy of the molecule as a function of the relative positions of the atomic coordinates by successive iterations with a block-diagonalized Newton–Raphson least-squares algorithm[55] is given in eq A1 with the components defined in eqs A2–A6.

$$E_{TOT} = \sum_{i=1}^{5} \sum E_i \tag{A1}$$

$$E_1 = \tfrac{1}{2}K_s(l - l_0)^2 + K_s'(l - l_0)^3 \tag{A2}$$

$$E_2 = (0.043828)\tfrac{1}{2}K_b(\theta - \theta_0)^2 + K_b'(\theta - \theta_0)^4 \tag{A3}$$

$$E_3 = \tfrac{1}{2}V_1(1 + \cos\omega) + \tfrac{1}{2}V_2(1 - \cos 2\omega) + \tfrac{1}{2}V_3(1 + \cos 3\omega) \tag{A4}$$

$$E_4 = \epsilon^*((2.90 \times 10^5)\exp(-12.5(r/r^*)) - 2.25(r^*/r)^6) \tag{A5}$$

$$E_5 = (14.39418)\frac{\mu_i\mu_j}{DR_{ij}^3}(\cos\chi - 3\cos\alpha_i\alpha_j) \tag{A6}$$

E_1 represents the bond deformation energies, K_s is the derived stretching force constant (mdyn/Å), K_s' is the anharmonic correction stretching force constant (2.0 mdyn/Å, default value[55]), while l and l_0 are the actual and ideal bond lengths (Å), respectively. E_2 accounts for the angle deformation strain contributions, where 0.043828 is a conversion factor (mdyn·Å/rad^2/molecule to kcal/deg^2/mole), K_b is the angle bending force constant (7×10^{-8} mdyn·Å/rad^2 default value[55]), while θ and θ_0 are the actual and ideal bond angles (deg), respectively. E_3 is the strain energy contribution from each torsional angle deformation, with V_1, V_2, and V_3 the 1-, 2-, and 3-fold torsional constants (kcal·mol^{-1}) that determine the variation in torsional strain energy as a function of the dihedral angle ω (deg). The nonbonded (van der Waals) energy for the interactions of all atom pairs *ik*

(110) Munro, O. Q.; Marques, H. M. Unpublished work.

(in ≥1,4 relationships) is given by E_4, where $\epsilon^* = (\epsilon_i\epsilon_k)^{1/2}$ with ϵ_i and ϵ_k representing the "hardness" of atoms i and k (kcal·mol^{-1}), $r^* = r_i + r_k$, the sum of the van der Waals radii of atoms i and k (Å), and r is the distance between the two atoms (Å). When $r^*/r > 3.311$, eq A5 reduces to $E_5 = \epsilon^*(336.176)r^*/r$ to prevent two atoms fusing when they come very close together. E_6 is the dipole interaction energy, where μ_i and μ_j are the bond moments (D) of two bonds close in space, χ is the angle between the dipoles (deg), R is the line between midpoints of the bonds, α_i and α_j are the angles (deg) between the dipole axes and the lines along which R is measured, 14.39418 converts ergs·molecule^{-1} to kcal·mol^{-1}, and D is the dielectric constant (default value = 1.5).

Registry No. Ni(porph), 15200-33-6; Fe(porph), 15213-42-0; Zn(porph), 137626-05-2; Pb(porph), 30993-25-0; $[P(TPP)(OH)_2]^+$, 87374-07-0; Ni(OEP), 24803-99-4; Fe(TPP), 16591-56-3; Zn(TPP), 14074-80-7; Pb(TPrP), 73395-80-9.

Supplementary Material Available: Listing of selected observed and MM-calculated bond lengths, bond angles, and torsional angles and a listing of modifications made to the MM2(87) program (42 pages). Ordering information is given on any current masthead page.

Theoretical Increments and Indices for Reactivity, Acidity, and Basicity within Solid-State Materials

Richard Dronskowski[†]

Contribution from the Department of Chemistry and Materials Science Center, Cornell University, Ithaca, New York 14853-1301. *Received November 27, 1991*

Abstract: With the aim of aiding the design of solid-state chemical syntheses, we construct some quantum mechanical indicators of reactivity, acidity, and basicity in crystal chemistry. These definitions are based on three-dimensional electronic structure calculations. After referring back to the concept of density-functional theory of Kohn and Sham and, in particular, the definition of absolute hardness due to Parr and Pearson, we first give a short overview of what is known in the field of molecular quantum chemistry. We then proceed to derive local *reactivity*, *electrophilicity* (acidity), and *nucleophilicity* (basicity) increments and indices both for atoms and bonds in any possible crystal structure. Our definitions are formulated in terms of a one-electron picture, and the first concrete calculations are performed within the framework of the semiempirical extended Hückel tight-binding method. However, the definitions are not restricted to the latter method and are quite easily generalized for ab initio numerical techniques to solve the complex eigenvalue problem in k-space. As an illustrative application, we investigate the acid–base solid-state reaction from $K_2Ti_4O_9$ to $K_2Ti_8O_{17}$. A comparison of our approach, which is suited (but not restricted) to the solid state, with another scheme from molecular orbital calculations is attempted. In detail, we (i) determine the compound's resistance to electronic attack for different electron counts, (ii) analyze all atoms with respect to their electronic reactivity, acidity, and basicity, and (iii) clearly identify the chemically most basic oxygen atom by its outstanding *atomic nucleophilicity* (basicity) *index*. In fact, the changing connectivity of this single O atom governs the structural change from $K_2Ti_4O_9$ to $K_2Ti_8O_{17}$. We perform a numerical investigation of Rouxel's hypothesis that the basicity of this particular O atom could be decreased by replacing one Ti atom by a Nb atom, and finally we elucidate the resulting changes in the electronic structure in detail.

1. Introduction

Even though the comparatively young discipline of solid-state inorganic chemistry has made great progress during the last three decades, there still seems to be a strange discrepancy in its methodology.

On one hand, modern solid-state chemistry is unthinkable without X-ray crystal structure analysis, which allows a detailed and unambiguous description of the geometry and stoichiometry of the often complex chemical structures. Therefore, one might well take the view that these huge molecules synthesized by solid-state chemists are at least as well characterized as the "typical" small molecules of solution chemistry, whose structures are often determined by various spectroscopic techniques, as well as by crystallography in the solid state.

On the other hand, a solid-state chemist engaged in generating three-dimensional periodic structures can *plan* the individual synthetical steps only in a very rudimentary way and must often rely on the classical "shake and bake" techniques.[1] While organic chemistry faces up each day to incredibly complicated organic (natural or unnatural) molecules whose syntheses are *planned step by step*, an even approximately similar strategy to retrosynthesis,[2,3] for example, seems to be out of the question for inorganic solid-state chemistry. As a matter of fact, there is no simple *Ansatz* in sight to predict nontrivial reaction paths toward *imagined* structures.

Besides the greater elemental variety of solid-state chemistry compared to organic chemistry, there is another fundamental reason for this finding. The majority of solid-state inorganic compounds is, in fact, only stable in the solid phase. This might sound trivial, but in reality it represents a singularity compared to the behavior of molecules that arise from solution chemistry. A typical giant solid-state molecule showing fascinating structural details in the crystal *decomposes* at the melting point because its chemical bonding is intimately connected to the ordered crystalline state. Thus, the confinement to a single small unit (the *molecule*), which is so successful in organic synthesis, does not seem to work. In addition, there is obviously no easy way to see or define a "functional group" in a solid-state compound, although this concept is so extremely important in organic synthesis. Even worse, one has to face the sad fact that solid-state counterparts to "functional group interconversions" or "synthons" are extremely rare.

What is retained in inorganic as well as in organic chemistry, in the solid state or in solution, is the time-honored and useful concept of acidity and basicity, except that this idea, and its

[†] Present address: Max-Planck-Institut für Festkörperforschung, Heisenbergstr. 1, 7000 Stuttgart 80, Germany.

(1) Rouxel, J. *Giving the Baker lectures at Cornell University*, 1991.
(2) Corey, E. J. *Angew. Chem.* **1991**, *103*, 469–479; *Angew. Chem., Int. Ed. Engl.* **1991**, *30*, 455–465.
(3) Warren, S. *Organic Synthesis: The Disconnection Approach*; John Wiley: Chichester, New York, 1982.

0002-7863/92/1514-7230$03.00/0